

# Cu-catalysed enantioselective radical heteroatomic S–O cross-coupling

Received: 23 February 2022

Accepted: 27 October 2022

Published online: 27 December 2022



Yong-Feng Cheng<sup>1,6</sup>, Zhang-Long Yu<sup>1,6</sup>, Yu Tian<sup>1,6</sup>, Ji-Ren Liu<sup>2,3,4,6</sup>, Han-Tao Wen<sup>1</sup>, Na-Chuan Jiang<sup>1</sup>, Jun-Qian Bian<sup>1</sup>, Guo-Xiong Xu<sup>2,3,4</sup>, Dan-Tong Xu<sup>1</sup>, Zhong-Liang Li<sup>5</sup>, Qiang-Shuai Gu<sup>5</sup>✉, Xin Hong<sup>2,3,4</sup>✉ & Xin-Yuan Liu<sup>1</sup>✉

The transition-metal-catalysed cross-coupling reaction has established itself as one of the most reliable and practical synthetic tools for the efficient construction of carbon–carbon (*p*-block elements other than carbon) bonds in both racemic and enantioselective manners. In contrast, development of the corresponding heteroatom–heteroatom cross-couplings has so far remained elusive, probably due to the under-investigated and often challenging heteroatom–heteroatom reductive elimination. Here we demonstrate the use of single-electron reductive elimination as a strategy for developing enantioselective S–O coupling under Cu catalysis, based on both experimental and theoretical results. The reaction manifests its synthetic potential by the ready preparation of challenging chiral alcohols featuring congested stereocentres, the expedient valorization of the biomass-derived feedstock glycerol, and the remarkable catalytic 4,6-desymmetrization of inositol. These results demonstrate the potential of enantioselective radical heteroatomic cross-coupling as a general chiral heteroatom–heteroatom formation strategy.

The transition-metal-catalysed cross-coupling reaction between an organo(pseudo)halide and a nucleophile is important in organic synthesis for carbon–carbon (C–C) and carbon–heteroatom (C–E, where E indicates *p*-block elements other than carbon) bond formations, in both industrial and academic settings (Fig. 1a)<sup>1</sup>. By invoking organometallic chemistry, the reaction is imparted not only with new reactivities beyond the innate capacities of its substrates, but also with handles for chemo- and stereoselectivity control via ligand tuning. Of particular interest is the recent great progress made in developing the enantioselective variant of transition-metal-catalysed C–C cross-coupling<sup>2,3</sup> and the emerging efforts in exploring enantioselective C–E cross-coupling<sup>4–8</sup>. In stark contrast, synthetic methodologies

for the corresponding transition-metal-catalysed heteroatom–heteroatom (E–E') cross-coupling between a heteroatomic (pseudo) halide and a heteroatomic nucleophile has so far remained largely underexplored<sup>9</sup>, and its enantioselective variant, to the best of our knowledge, is unknown. This is despite the fact that transition-metal-catalysed E–E' formation reactions are well known<sup>10–13</sup>. The challenge seems to mainly rest on the final reductive elimination step, because the oxidative addition with a heteroatomic electrophile<sup>14</sup> and the ligand exchange with a heteroatomic nucleophile<sup>15,16</sup> have been well reported for transition-metal-catalysed C–E cross-coupling. In fact, concerted two-electron E–E' reductive elimination has been only sporadically proposed<sup>17,18</sup>, and such a process probably becomes

<sup>1</sup>Shenzhen Grubbs Institute and Department of Chemistry, Guangdong Provincial Key Laboratory of Catalysis, Southern University of Science and Technology, Shenzhen, China. <sup>2</sup>Center of Chemistry for Frontier Technologies, Department of Chemistry, State Key Laboratory of Clean Energy Utilization, Zhejiang University, Hangzhou, China. <sup>3</sup>Beijing National Laboratory for Molecular Sciences, Beijing, China. <sup>4</sup>Key Laboratory of Precise Synthesis of Functional Molecules of Zhejiang Province, School of Science, Westlake University, Hangzhou, China. <sup>5</sup>Academy for Advanced Interdisciplinary Studies and Department of Chemistry, Southern University of Science and Technology, Shenzhen, China. <sup>6</sup>These authors contributed equally: Yong-Feng Cheng, Zhang-Long Yu, Yu Tian, Ji-Ren Liu. ✉e-mail: [guqs@sustech.edu.cn](mailto:guqs@sustech.edu.cn); [hchem@zju.edu.cn](mailto:hchem@zju.edu.cn); [liuxy3@sustech.edu.cn](mailto:liuxy3@sustech.edu.cn)

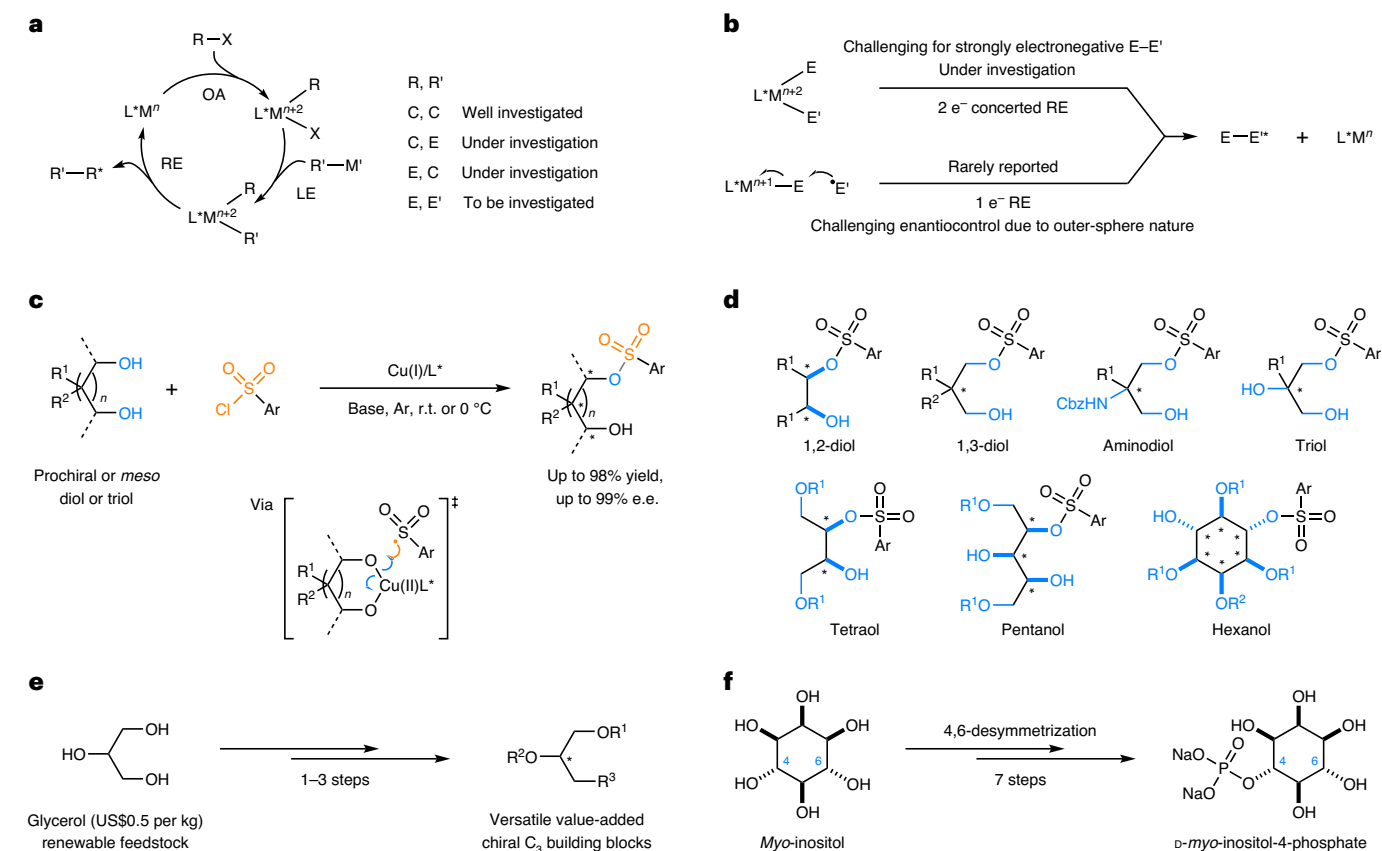


**Fig. 1 | Challenges and development of transition-metal-catalysed enantioselective heteroatom–heteroatom cross-coupling.** **a**, An outline of the mechanism and overview of transition-metal-catalysed enantioselective cross-coupling. OA, oxidative addition; LE, ligand exchange; RE, reductive elimination; E, *p*-block elements other than carbon. **b**, Challenge for realizing E–E' cross-coupling via enantioselective RE from transition-metal complexes. **c**, Copper-

catalysed enantioselective S–O cross-coupling via single-electron RE. Ar, argon. **d**, A broad scope of enantioenriched products (>50 examples, with compounds containing up to six stereocentres) are formed in this study. **e**, Practical and expedient transformation of glycerol to a panel of highly synthetically useful chiral synthons. **f**, The achievement of highly enantioselective 4,6-desymmetrization of *myo*-inositol.

thermodynamically and/or kinetically challenging for two strongly electronegative heteroatoms<sup>19–21</sup> (Fig. 1b, top). Alternatively, single-electron reductive elimination may be energetically favourable due to the involvement of only one transition metal–heteroatom (M–E) bond break<sup>22–25</sup>. Nonetheless, such a mechanistic scenario has rarely been described for E–E' bond formation. More importantly, its outer-sphere nature in an intermolecular setting has long been known to render the enantiocontrol challenging<sup>26,27</sup> (Fig. 1b, bottom).

On the other hand, E–E' bonds, though greatly underrepresented in organic chemistry, are indispensable motifs in many valuable synthetic intermediates<sup>28</sup>, natural products<sup>29</sup>, bioactive molecules and drugs<sup>30</sup>. With the recently boosted development of *p*-block element chemistry, they have also become essential moieties in many novel catalysts and materials<sup>31,32</sup>. In this sense, the development of general and practical transition-metal-catalysed enantioselective E–E' cross-coupling would provide a robust and versatile synthetic platform to support research in multiple disciplines.

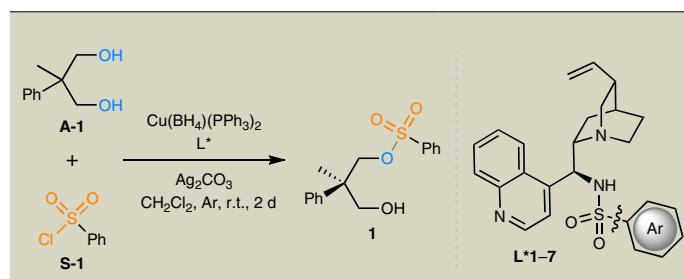
To this end, in this Article we describe a copper-catalysed enantioselective S–O coupling reaction that probably proceeds through a rare single-electron E–E' reductive elimination, on the basis of experimental and theoretical studies (Fig. 1c). The reaction leads to the successful desymmetrization of a variety of prochiral or *meso* diols or triols. Accordingly, a panel of highly enantioenriched 1,2-diol, 1,3-diol, 2-amino-1,3-diol, triol, tetraol, pentanol and hexanol scaffolds with up to six stereocentres are efficiently constructed, in particular those synthetically challenging acyclic all-carbon quaternary as well as nitrogen- and oxygen-bearing tetrasubstituted carbon

stereocentres (Fig. 1d). More importantly, the reaction is able to readily transform the prochiral renewable feedstock glycerol into a number of high-value-added chiral C<sub>3</sub> building blocks when coordinated with additional one- or two-step manipulations (Fig. 1e). In addition, the challenging 4,6-desymmetrization of *myo*-inositol is achieved using this reaction as the key step, culminating in the synthesis of D-*myo*-inositol-4-phosphate (Fig. 1f).

## Results and discussion

### Reaction development

Our group has been investigating copper-catalysed asymmetric transformations involving radical intermediates<sup>33</sup>. Recently, we have discovered that a series of multidentate chiral anionic ligands greatly enhance the single-electron reduction of alkyl halides by copper(I) for generating alkyl radical species, which readily participate in enantioselective C–C cross-coupling reactions<sup>25,34</sup>. Similar to alkyl halides, sulfonyl chlorides have been widely demonstrated as good sulfonyl radical precursors<sup>35</sup>. In addition, sulfonyl groups have been broadly used as both excellent activation and good protection groups for alcohols in organic synthesis<sup>36</sup>. As such, we wondered whether our copper(I)/chiral anionic ligand catalysts would promote enantioselective S–O cross-coupling between prochiral or *meso* diols or polyols and sulfonyl chlorides to provide a practical complementary approach for existing alcohol desymmetrization methodologies<sup>37</sup>. In particular, the construction of acyclic quaternary all-carbon stereocentres from acyclic substrates through an intermolecular desymmetrization reaction is synthetically appealing but has so far remained largely out of

**Table 1 | Results of initial ligand screening**


Entry	L*	Ar	Yield of <b>1</b> (%)	E.e. of <b>1</b> (%)
1	<b>L*1</b>	Ph	49	47
2	<b>L*2</b>	4-OMePh	34	45
3	<b>L*3</b>	4-NO <sub>2</sub> Ph	29	31
4	<b>L*4</b>	2,3,4,5,6-Me <sub>5</sub> Ph	83	83
5	<b>L*5</b>	3,5-(CF <sub>3</sub> ) <sub>2</sub> Ph	54	26
6	<b>L*6</b>	2,4,6- <sup>i</sup> Pr <sub>3</sub> Ph	84	79
7	<b>L*7</b>	1-Naphthyl	48	43

Reaction conditions: **A-1** (0.050 mmol), **S-1** (1.2 equiv.), Cu(BH<sub>4</sub>)(PPh<sub>3</sub>)<sub>2</sub> (10 mol%), L\* (10 mol%) and Ag<sub>2</sub>CO<sub>3</sub> (0.60 equiv.) in CH<sub>2</sub>Cl<sub>2</sub> (0.10 M) at r.t. for 2 d; yield was based on <sup>1</sup>H NMR analysis of the crude product using CH<sub>2</sub>Br<sub>2</sub> as an internal standard; e.e. values were based on chiral HPLC analysis.

reach for catalysts other than enzymes due to the enhanced conformational flexibility of the substrates<sup>38</sup>. Accordingly, at the beginning, we targeted prochiral acyclic 1,3-diols bearing a quaternary carbon tether<sup>39</sup>, which have proved to be poor substrates in many established desymmetrization methods with low reactivity and/or unsatisfactory enantioselectivity. Thus, prochiral 1,3-diol **A-1** was reacted with benzenesulfonyl chloride (**S-1**) in the presence of Cu(BH<sub>4</sub>)(PPh<sub>3</sub>)<sub>2</sub> and a panel of chiral cinchona alkaloid-derived sulfonamide ligands **L\*1–L\*7** (Table 1) under an argon atmosphere. Additional Ag<sub>2</sub>CO<sub>3</sub> was added to quench the stoichiometric amount of HCl generated in situ. Under these conditions, ligands **L\*4** (entry 4) and **L\*6** (entry 6), featuring sterically bulky aryl groups in the sulfonamide moieties, gave both high yield and good enantioselectivity. Further systematic reaction-condition optimization (Supplementary Table 1) led to the identification of the optimal conditions as follows: 1.2 equiv. **S-1**, 10 mol% CuI, 10 mol% **L\*4** (for the X-ray structure of this ligand with its absolute configuration, see Supplementary Fig. 18), 0.60 equiv. Ag<sub>2</sub>CO<sub>3</sub>, and 20 mol% proton sponge in CHCl<sub>3</sub> at 0 °C (for experimental results concerning the effect of the silver carbonate and proton sponge, see Supplementary Table 2). Under the optimal conditions, the desired product **1** was obtained in 86% yield with 94% e.e. (Table 2).

### Substrate scope

The subsequent examination of various arylsulfonyl chlorides revealed good tolerance of a variety of substituents (**1–10**) with distinct electronic and/or steric properties (Table 2). Of particular note is the compatibility of benzene- (BsCl for **1**), *p*-toluene- (*p*-TsCl for **2**) and *p*-nitrobenzenesulfonyl chlorides (*p*-NsCl for **9**), which are routinely utilized in organic synthesis, paving the way for versatile follow-up transformations. As for the scope of 2,2-dicarbofunctionalized 1,3-diols (Table 2), good yield and excellent enantioselectivity were observed, as long as the 2-aryl-2-alkyl substitution pattern was maintained (**11–28**). A number of functional groups, particularly those potentially reactive ones such as acetal (**17**), organohalides (**15**, **23** and **24**), alkenes (**18** and **19**) and alkynes (**20** and **21**), on either the 2-aryl or 2-alkyl substituents, were well tolerated under the reaction conditions. A heterocyclic 2-(3-thiophenyl) ring (**29**) was compatible with the reaction. Strikingly, the 2-aryl ring could be replaced with an ester group (**30**), which

led to moderate yield and good enantioselectivity. Furthermore, a 2-oxindole-derived 1,3-diol was also applicable to the reaction, furnishing product **31** in 85% yield with 85% e.e. Interestingly, *meso* 1,2-diol was also suitable for this reaction, affording the chiral coupling product **32** with excellent results.

To further strengthen the synthetic utility of this methodology, we next switched to the enantioselective coupling of a series of prochiral serinol derivatives (Fig. 2a), given the importance of chiral 1,2-amino alcohol skeletons, especially those containing N-bearing tetrasubstituted carbon stereocentres. Noteworthy is that non-enzymatic desymmetrization of these prochiral 1,3-diols, although synthetically attractive, has only rarely been achieved with a reasonably wide substrate scope<sup>40–43</sup>. The initial poor results with benzyloxycarbonyl (Cbz)-protected serinol under the aforementioned optimal conditions stimulated us to reoptimize the reaction conditions (Supplementary Table 3). Surprisingly, the use of the superior ligands **L\*4** and **L\*6** for 2,2-dicarbo-substituted 1,3-diol substrates proved to be detrimental to the serinol substrate in terms of both reaction efficiency and enantioselectivity. By contrast, the originally poor ligands **L\*3** and **L\*5** bearing electron-deficient aryl groups in the sulfonamide moieties provided obviously enhanced enantioselectivity compared with **L\*1** for the serinol substrate. These results indicate remarkable changes in the enantiodetermining transition states, possibly as a result of different coordination modes of these two types of substrate to the copper catalysts (for examples, see Supplementary Fig. 5). Interestingly, **L\*8** bearing an additional quinoline N-binding site gave rise to substantially boosted enantioselectivity as well as reaction yield, thus highlighting the importance of ligand-binding modes in dictating the overall reaction performance. Further screening of other reaction parameters with **L\*8** led to appropriate conditions that delivered the desired S–O coupling products **33–41** in moderate to good yield with high e.e., and good functional group compatibility was again observed. The tolerance of a heterocyclic triazole ring was further achieved by replacing **L\*8** with **L\*9** to afford product **42**. Notably, the Cbz-protected immunomodulating drug fingolimod (for treating multiple sclerosis) was also a suitable substrate for the reaction to provide enantioenriched product **43**. This compound can be a good starting material for preparing useful chiral derivatives of fingolimod, such as its phosphorylated derivative fingolimod-P, the real agonist for multiple sphingosine 1-phosphate (S1P) receptor subtypes. The synthetic potential was further demonstrated by converting coupling product **34** to chiral thioether **44** and phosphine **45** in one nucleophilic attack step (Fig. 2b, left). More importantly, valuable α,α-disubstituted chiral unnatural α-amino acid **46** was readily obtained by straightforward nucleophilic attack, acidic hydrolysis and alcohol oxidation, in three steps from **34** (Fig. 2b, right).

Besides the 1,2- or 1,3-diols mentioned above, the reaction is also applicable to 1,2,3-triols for the expedient access of O-bearing tetrasubstituted carbon stereocentres<sup>44–47</sup>, the last major type of sterically congested stereocentre in natural products and drug molecules. Thus, a diverse range of substituents at the carbon-2 positions of 1,2,3-triols (**47–55**) were well tolerated under the original optimized conditions for diols (Fig. 2c). Further treatment of the chiral alcohol products **52–54** with a base efficiently provided highly enantioenriched epoxides **56–58** (Fig. 2d, left). The presence of a triazole nucleophile during the latter base treatment directly led to the intermolecular displacement product **59** (Fig. 2d, right), which is an important synthetic intermediate towards antifungal agents ZD0870 and Sch45450<sup>48</sup>.

The valorization of biomass-derived compounds such as polyols is of vital importance for the development of biomass resources as renewable and sustainable substituents for fossil fuels, of which the use has long been fraught with depletion and environmental concerns. In this regard, the biomass platform molecule glycerol, the by-product of biodiesel production on an industrial scale, has been the subject of an abundance of efforts for its conversion to commodities and specialty chemicals<sup>49</sup>. Nonetheless, the transformation of glycerol into

**Table 2 | Substrate scope for sulfonyl chlorides and prochiral 2,2-disubstituted 1,3-diols as well as a *meso* 1,2-diol**

Diols	Sulfonyl chlorides
<b>Sulfonyl chloride</b> 	
<b>1</b>	86%, 94% e.e.
<b>2</b>	86%, 93% e.e.
<b>3</b>	57%, 92% e.e.
<b>4</b>	67%, 93% e.e.
<b>5</b>	56%, 91% e.e.
<b>6</b>	87%, 91% e.e.
<b>7</b>	98%, 95% e.e.
<b>8</b>	97%, 94% e.e.
<b>9</b>	81%, 94% e.e.
<b>10</b>	72%, 91% e.e.
<b>2,2-Disubstituted 1,3-diol &amp; <i>meso</i> 1,2-diol</b> 	
<b>11</b>	92%, 93% e.e.
<b>12</b>	88%, 94% e.e.
<b>13</b>	89%, 96% e.e.
<b>14</b>	80%, 93% e.e.
<b>15</b>	67%, 89% e.e.
<b>16</b>	97%, 98% e.e.
<b>17</b>	82%, 93% e.e.
<b>18</b>	88%, 95% e.e.
<b>19</b>	81%, 97% e.e.
<b>20</b>	94%, 95% e.e.
<b>21</b>	87%, 95% e.e.
<b>22</b>	78%, 84% e.e.
<b>23</b>	75%, 88% e.e.
<b>24</b>	80%, 85% e.e.
<b>25</b>	55%, 84% e.e.
<b>26</b>	74%, 94% e.e.
<b>27</b>	77%, 92% e.e.
<b>28</b>	86%, 94% e.e.
<b>29</b>	72%, 91% e.e.
<b>30</b>	42%, 79% e.e.
<b>31</b>	85%, 85% e.e.
<b>32</b>	97%, 95% e.e.

Reaction conditions: alcohol (0.30 mmol), sulfonyl chloride (1.2 equiv.), CuI (10 mol%), **L\*4** (10 mol%), Ag<sub>2</sub>CO<sub>3</sub> (0.60 equiv.) and proton sponge (20 mol%) in CHCl<sub>3</sub> (3.0 ml) under Ar at 0 °C for 2 d; yield was isolated; e.e. values were based on chiral HPLC analysis.

high-value-added chiral building blocks has so far remained largely underdeveloped. To the best of our knowledge, the only known asymmetric catalytic transformation was achieved by the kinetic resolution of the initial desymmetrization products for high enantioselectivity under scaffolding catalysis<sup>50</sup>. Accordingly, we next switched our attention to the desymmetrization of glycerol (Fig. 3a). Fortunately, the desired product **60** was obtained from chemically pure glycerol in 75% yield and 93% e.e. under the standard conditions for 1,2,3-triol substrates. The subsequent one- or two-step manipulations of **60** readily afforded highly enantioenriched building blocks glycidol (**61**), epichlorohydrin (**62**), tosylated glycerol carbonate (**63**), solketal tosylate (**64**) and azidoglycerol (**65**), all of which are heavily utilized in asymmetric organic synthesis. Furthermore, tosylate **60** itself is already an excellent synthetic building block—the cough suppressant drug levodropropizine (**66**) can be smoothly synthesized from it in one step. In addition, the crude filtrate of the reaction for generating **60** could be directly utilized for the following intermolecular displacement, delivering drug **66** without any loss of enantioselectivity. Noteworthy is that the much less expensive crude glycerol (~71% purity) could be directly employed in this reaction to give **60** in practically reasonable yield with only slightly diminished enantioselectivity (Fig. 3b). In addition, the antipode of **60** was readily prepared using the pseudo-enantiomer of ligand **L\*4** (**L\*4'**), in good yield and high e.e.

(Fig. 3c). Besides glycerol, the desymmetrization of the readily commercially available biomass-derived sugar alcohols erythritol and xylitol were achieved under slightly modified conditions using their bis-pivalate derivatives **A-3** and **A-4**, respectively (Fig. 3d,e; for reaction-condition optimization, see Supplementary Tables 4 and 5).

Another noteworthy biomass-derived polyol is *myo*-inositol, which features up to a total of six prochiral stereocentres with a low cost close to that of glucose. It has thus been broadly utilized as a starting material for the synthesis of a range of natural products, particularly the biologically important chiral inositol phosphates<sup>51</sup>. Nonetheless, the desymmetrization of this molecule has largely hinged on chiral auxiliary-based resolutions<sup>51</sup>, and asymmetric catalytic methods have been achieved only by the Miller group<sup>52</sup>. Notably, they have accomplished the 1,3-desymmetrization of a 2,4,6-protected *myo*-inositol by peptide-catalysed enantioselective sulfonylation<sup>53</sup>. However, the 4,6-desymmetrization has proved to be challenging due to the high stereochemical similarity between the two stereocentres immediately flanking each of the two positions. Accordingly, only poor to moderate enantioselectivity has been obtained in the 4,6-desymmetrization of *myo*-inositol derivatives under peptide catalysis<sup>54</sup>. To this end, we managed to identify **L\*11** as the optimal ligand (in contrast to other ligands employed in this work, we consider this ligand as a neutral tridentate *N,N,N*-ligand; for brief discussions in this regard, see the



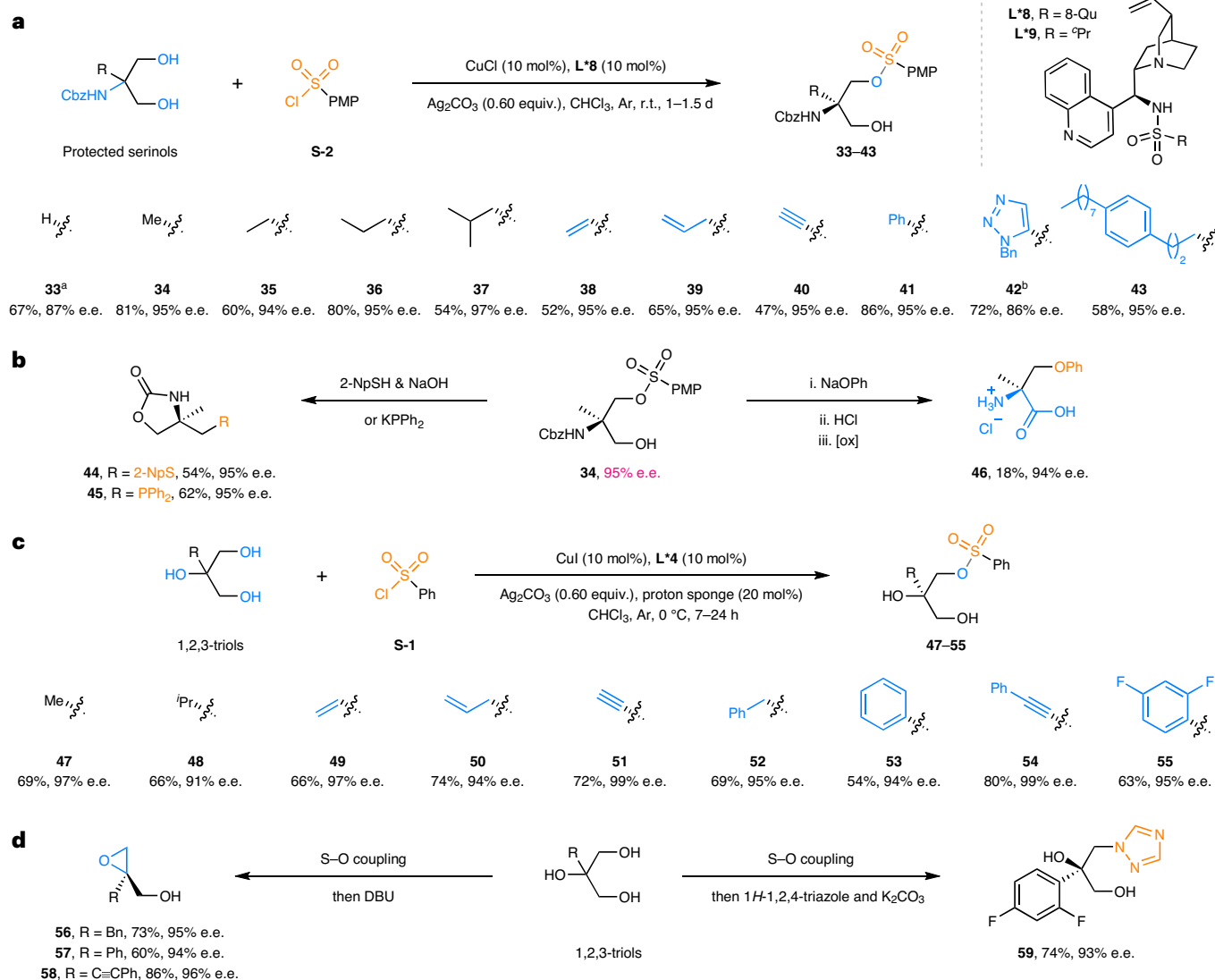


**Fig. 2 | Substrate scope and synthetic applications.** **a**, Scope for 2-amino-1,3-diols. Cbz, benzyloxycarbonyl; PMP, *para*-methoxyphenyl; 8-Qu, 8-quinolyl; <sup>i</sup>Pr, cyclopropyl. **b**, Further one- or three-step manipulations of the thus-obtained **34** led to enantioenriched thioether **44**, phosphine **45** and  $\alpha,\alpha$ -disubstituted unnatural  $\alpha$ -amino acid **46**. **c**, Scope for 1,2,3-triols. **d**, Further

treatment of **52–55** with a base afforded enantioenriched quaternary epoxides **56–58**, and the introduction of a triazole nucleophile during the base treatment provided compound **59**, an important synthetic intermediate towards antifungal agents. DBU, 1,8-diazabicyclo[5.4.0]undec-7-ene. <sup>a</sup>Proton sponge (5.0 mol%). <sup>b</sup>L\*9 (10 mol%).

mechanistic and computational study sections in Supplementary Information) for the Cu(I)-catalysed enantioselective S–O coupling to realize 4,6-desymmetrization of an inositol derivative **A-5** in 78% yield with 91% e.e. (Fig. 3f; for the reaction optimization, see Supplementary Table 6). The enantiopurity of product **69** was further boosted up to 98% e.e. after one round of recrystallization. Next, phosphorylation of **69** followed by three deprotection steps led to the formation of *D*-myo-inositol-4-phosphate (**70**) in 57% yield over four steps, with 99% e.e. The use of L\*11', the pseudo-enantiomer of L\*11, gave rise to the enantiomer of **69** (**69'**) in good yield with high enantioselectivity. The absolute configurations of **16** (Table 2 and Supplementary Fig. 19), **45** (Fig. 2b and Supplementary Fig. 20), **59** (Fig. 2d and Supplementary Fig. 21) and **69** (Fig. 3f and Supplementary Fig. 22) were determined by X-ray crystallographic analysis, and those of other related products were assigned by analogy accordingly.

### Mechanistic studies

To gain insight into the reaction mechanism, we first carried out radical inhibition experiments with (2,2,6,6-tetramethylpiperidin-1-yl)

oxyl (TEMPO), 1,4-benzoquinone or butylated hydroxytoluene (BHT), respectively, all of which demonstrated remarkable reaction inhibition (Fig. 4a and Supplementary Fig. 1). In particular, the reaction with BHT produced **71** and **72** (for the X-ray structure of **72**, see Supplementary Fig. 23), probably resulting from the trapping of conceivable sulfonyl radicals by BHT, in addition to the normal S–O coupling product **1** (Fig. 4a). The formation of sulfonyl radicals was further supported by the reaction with the radical clock probe **AE-1** in the absence of diol **A-1** under otherwise standard conditions (Fig. 4b), which provided the expected radical trap products **73** and **74** with the cyclopropane rings opened. This result also indicated that the generation of sulfonyl radicals can proceed without diol. To investigate the involvement of sulfonyl radicals in the product formation, we deliberately generated sulfonyl radicals using other known strategies<sup>35</sup>, which were also able to afford the corresponding S–O coupling products with diminished yet significant enantioselectivity, albeit of low yield (Fig. 4c; for results with allyl sulfone, thiosulfonate and sulfonyl hydrazide as sulfonyl radical precursors, see Supplementary Fig. 2). In contrast, much more unstable benzyl sulfonyl radicals<sup>36</sup> only underwent desulfonation to provide benzyl

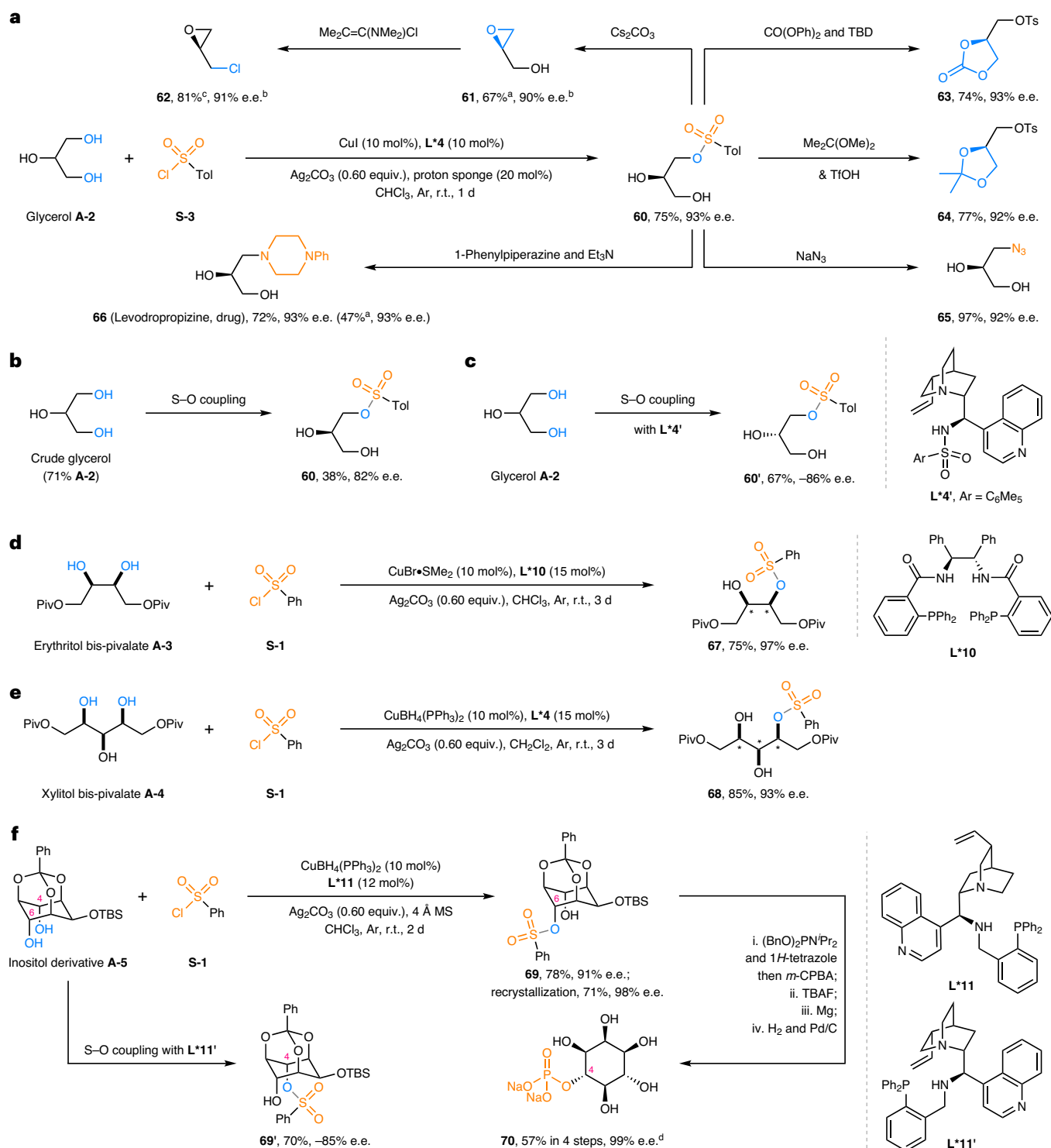


**Fig. 3 | Desymmetrization of polyols from natural resources.**

**a**, Desymmetrization of glycerol **A-2** was readily achieved, and the enantioenriched product **60** was converted to highly utilized synthons in organic synthesis and a drug molecule (**66**) via additional one- or two-step transformations. **b**, Crude glycerol was applicable for the reaction to deliver a practically reasonable yield and slightly diminished enantioselectivity of product **60**. **c**, Replacing **L\*4** with its pseudo-enantiomer **L\*4'** led to the enantiomer of **60** (**60'**) in good yield with high enantioselectivity. **d**, Desymmetrization of protected *meso* erythritol **A-3** was achieved using **L\*10** as the ligand under reoptimized conditions. **e**, Desymmetrization of protected

*meso* xylitol **A-4** was achieved using ligand **L\*4** under reoptimized conditions. **f**, 4,6-Desymmetrization of protected inositol **A-5** was fulfilled with ligand **L\*11** or its pseudo-enantiomer **L\*11'**, which led to enantioenriched product **69** or its enantiomer **69'**, respectively. Subsequent transformations of **69** gave rise to *D-myo*-inositol-4-phosphate **70** in four steps. <sup>a</sup>In two steps from glycerol with a filtration operation in between. <sup>b</sup>The e.e. value was determined on a one-step derivative. <sup>c</sup>NMR yield. <sup>d</sup>The e.e. value was determined on the synthetic precursor before hydrogenolysis. TBD, 1,5,7-triazabicyclo[4.4.0]dec-5-ene; Tol, *p*-tolyl; Ts, *p*-tosyl; Piv, pivaloyl; TBS, *tert*-butyldimethylsilyl; MS, molecular sieves; *m*-CPBA, *meta*-chloroperoxybenzoic acid; TBAF, tetra-*n*-butylammonium fluoride.

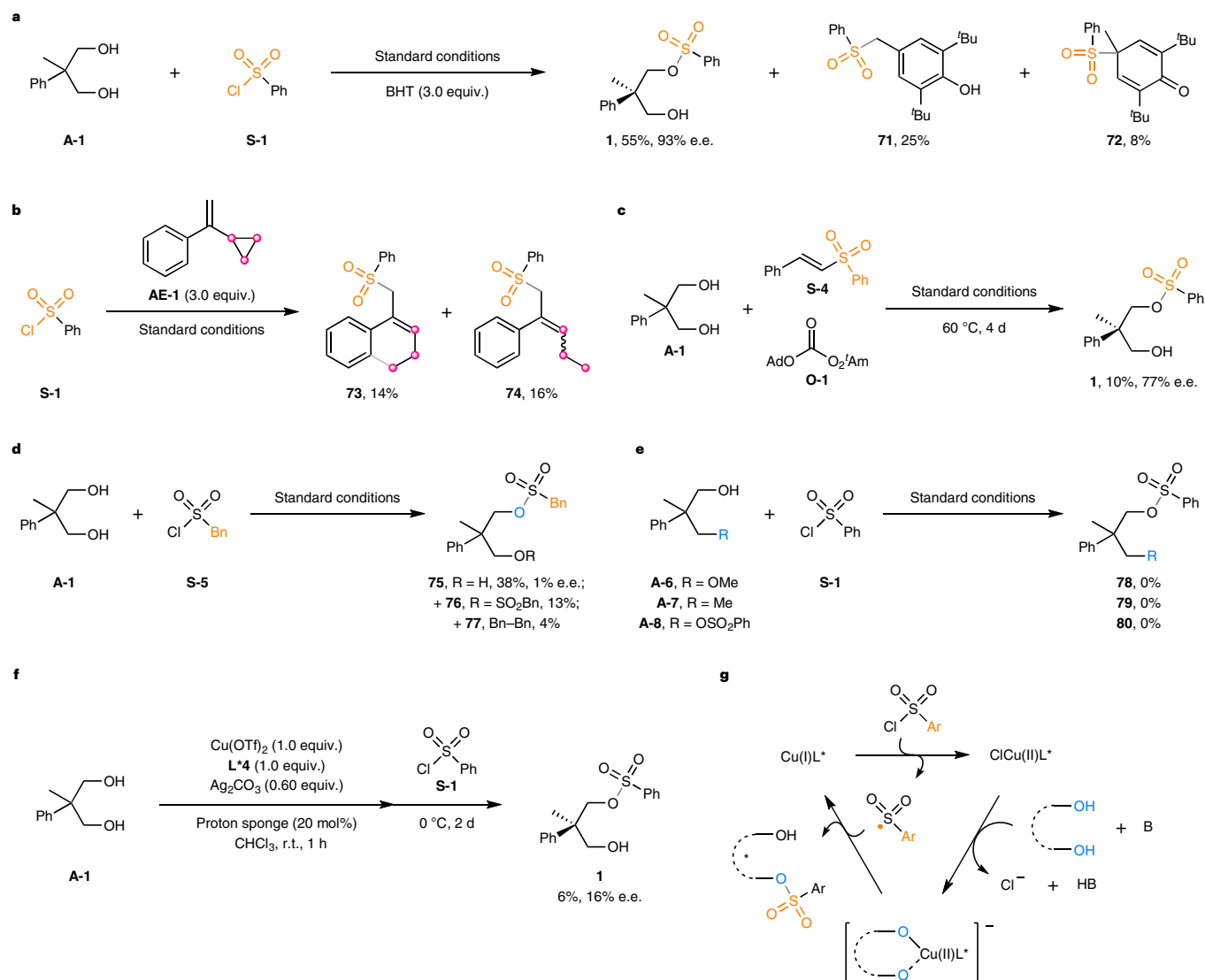


**Fig. 4 | Experimental mechanistic studies.** **a**, A radical inhibition experiment with BHT indicated reaction retardation and afforded sulfonyl radical-derived products **71** and **72**. BHT, butylated hydroxytoluene. **b**, Replacing **A-1** with a radical clock probe **AE-1** led to the formation of expected radical trap products **73** and **74**. **c**, Using an alternative method for generating sulfonyl radical also gave rise to the copper-catalysed enantioselective S–O cross-coupling product. Ad, 1-adamantyl; <sup>t</sup>Am, *tert*-amyl. **d**, The benzyl sulfonyl radical underwent fast desulfonation and dimerization to afford **77**, and the non-stereoselective ionic sulfonylation reaction proceeded well via sulfene intermediates. **e**, Monoalcohols did not undergo the S–O cross-coupling reaction, suggesting the

necessary binding of both the two hydroxy groups to Cu and the irrelevance of product kinetic resolution in the reaction. **f**, The experiment with stoichiometric Cu(OTf)<sub>2</sub> and **L\*4** resulted in low yield and marginal enantioselectivity, probably excluding the Cu(II) Lewis acid-catalysed ionic sulfonylation pathway. **g**, The proposed working mechanism involves the single-electron oxidative addition of the Cu(I) catalyst to sulfonyl chlorides, subsequent ligand exchange of the thus-generated Cu(II) species with the diol substrates, and final single-electron reduction elimination between the sulfonyl radicals and the alkoxide complex. Standard conditions refer to that shown in Table 2.

radical homocoupling product **77** (Fig. 4d and Supplementary Fig. 3). At the same time, essentially racemic mono-sulfonylation product **75** was observed together with the bis-sulfonylation product **76**, both of which were probably formed through relatively fast non-stereoselective sulfonylation background reactions via sulfene intermediates (Supplementary Fig. 3)<sup>57</sup>. These results clearly supported an obligatory role of sulfonyl radicals in product formation. Next, we examined the alcohol-catalyst interaction mode by replacing one hydroxy group in **A-1** with a methoxyl, methyl or sulfonoxo group, which completely shut down the desired reactions (Fig. 4e). Thus, the binding of both the two hydroxy groups in the form of alkoxide to a possible Cu(II) catalytic species is probably necessary for the subsequent S–O coupling. The result of **A-8** also excluded the possible concurrent kinetic resolution of the desymmetrization product. We then tried to generate this envisioned

L\*Cu(II)–alkoxide complex by mixing stoichiometric amounts of a Cu(II) salt, **L\*4**, and **A-1**, which, upon exposure to sulfonyl chloride **S-1**, provided **1** in low yield with marginal enantioselectivity (Fig. 4f). Thus, an ionic sulfonylation pathway involving the direct reaction of such a chiral Cu(II) complex with sulfonyl chloride<sup>58</sup> seemed kinetically uncompetitive with the sulfonyl radical-mediated S–O coupling. On the basis of these results, a working mechanism was proposed, as shown in Fig. 4g. First, a single-electron oxidative addition between sulfonyl chlorides and the in situ-generated chiral L\*Cu(I) catalyst (for a high-resolution mass spectroscopy characterization, see Supplementary Fig. 4) provides sulfonyl radicals together with ClCu(II)L\*<sup>39</sup>. Next, in the presence of a base, this Cu(II) complex undergoes ligand exchange with the diol substrate to form the aforementioned L\*Cu(II)–alkoxide complex. Subsequent single-electron reductive elimination occurs

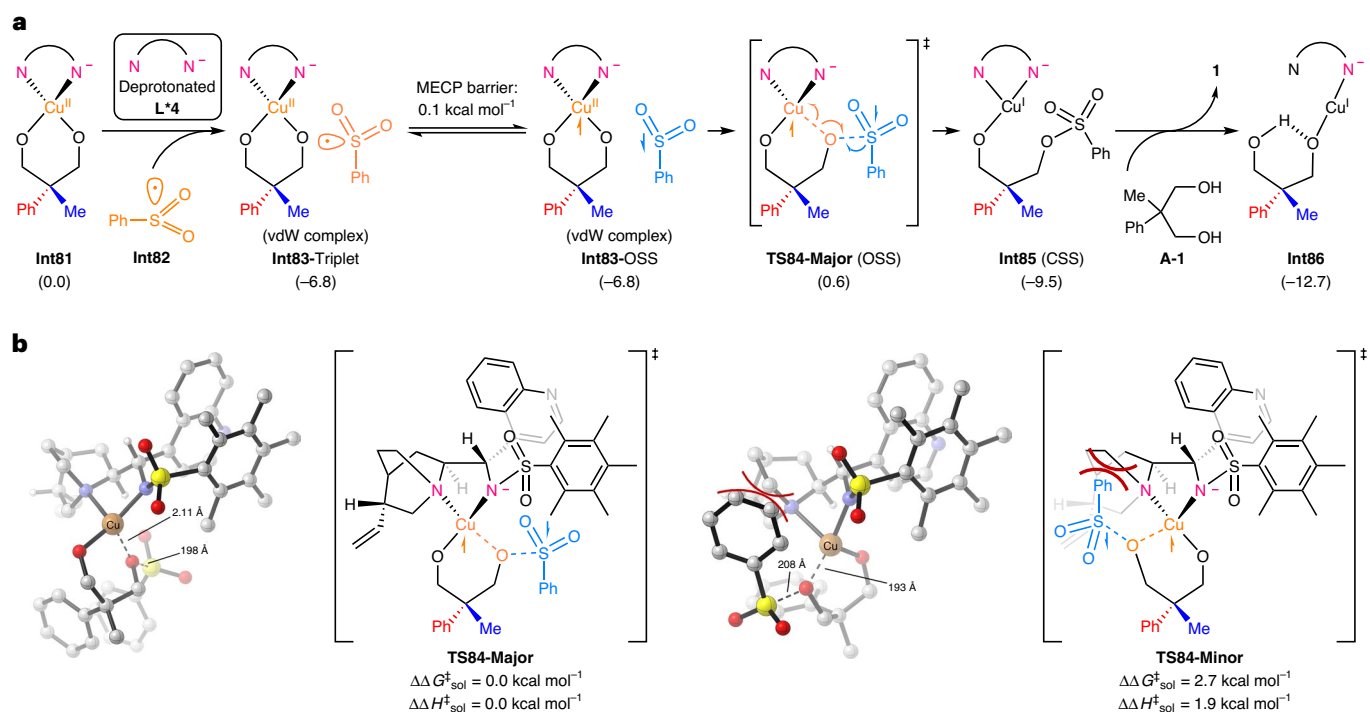


**Fig. 5 | Computational studies.** **a**, Mechanism for S-O bond formation. Sulfonyl radical **Int82** first complexes with **Int81** to form an anionic diradical species **Int83-Triplet**. **Int83-Triplet** can interconvert with the corresponding OSS state **Int83-OSS** through an MECP. S-O bond formation via an outer-sphere radical-substitution-type OSS transition state **TS84-Major** produces the sulfonylated product-coordinated CSS intermediate **Int85**. From **Int85**, the ligand exchange

liberates the desymmetrized product **1** and generates the copper(I) species **Int86**. DFT-computed free energies (in kcal mol<sup>-1</sup>) are shown in parentheses. **b**, Enantioselectivity-determining S-O bond formation transition states. This enantioselectivity control is due to the highlighted steric repulsion between the attacking sulfonyl radical and the quinuclidine moiety of the ligand. Trivial hydrogen atoms are omitted for clarity.

between sulfonyl radicals and the alkoxide complex, delivering the S-O coupling product.

We next explored the reaction mechanism and origins of enantioselectivity with density functional theory (DFT) calculations, using diol **A-1** and sulfonyl chloride **S-1** as model substrates and **L\*4** as model ligand. Through the Cu(I)-mediated inner-sphere electron transfer, the S-Cl bond of sulfonyl chloride is cleaved to generate the sulfonyl radical **Int82** (for details, see Supplementary Figs. 24–31, Supplementary Tables 13 and 17 and relevant text in Supplementary Information). Computational results on the S-O bond formation involving sulfonyl radical **Int82** are shown in Fig. 5a (Supplementary Table 12). **Int82** first complexes with the **L\*4Cu(II)**-alkoxide intermediate **Int81** (for details, see Supplementary Fig. 32 and relevant text in Supplementary Information) to form the anionic diradical van der Waals (vdW) complex **Int83-Triplet** (Supplementary Figs. 38–40). **Int83-Triplet** can readily interconvert with the corresponding open-shell singlet (OSS) state **Int83-OSS** through a minimum energy crossing point (MECP; Supplementary Fig. 35 and Supplementary Table 18). Subsequent outer-sphere radical-substitution-type open-shell singlet transition state **TS84-Major** produces the sulfonylated product-coordinated closed-shell singlet (CSS) intermediate complex **Int85**. Alternative mechanistic pathways of S-O bond formation are discussed in Supplementary Information (Supplementary Figs. 33–37). From **Int85**, the ligand exchange liberates the desymmetrized product **1** and generates the copper(I) active catalyst for the next catalytic cycle. Based on our calculations, the facile S-O bond formation requires a barrier of 7.4 kcal mol<sup>-1</sup> and determines the overall enantioselectivity of sulfonylation.

Our mechanistic model rationalizes the exceptional enantioselectivity control in the sulfonylation. Figure 5b compares the enantioisomeric S-O bond formation transition states **TS84-Major** and

**TS84-Minor**. **TS84-Major** is 2.7 kcal mol<sup>-1</sup> more favourable than **TS84-Minor**, which agrees well with the experimental observation (Table 2, entry 1, 94% e.e.). The chiral cinchona alkaloid-derived sulfonamide ligand coordinates to copper with the quinuclidine moiety and the deprotonated sulfonamide group, which differentiates the two alkoxide positions. In **TS84-Minor**, the attacking sulfonyl radical is proximal to the sterically demanding quinuclidine moiety, while such steric repulsions are alleviated in the favoured transition state **TS84-Major**. These steric repulsions are the leading factor of the enantioselectivity, and we also verified this mechanistic rationale with calculations of enantioselectivities on a truncated model (Supplementary Fig. 46). Conformational searches of the S-O bond formation transition state and verifications of the free energy preference under additional levels of theory are included in Supplementary Information (Supplementary Figs. 41–45 and Supplementary Tables 9–12, 19 and 20).

## Summary

We have developed a highly enantioselective heteroatomic S-O coupling reaction catalysed by Cu(I) together with a series of chiral multidentate ligands. This method provides a versatile and robust platform for the convenient construction of synthetically challenging acyclic all-carbon quaternary and N- and O-bearing tetrasubstituted stereocentres. More importantly, it allows for facile transformations of biomass-derived polyols, especially glycerol, into highly enantioenriched synthetic building blocks of great utility. It also provides a long-sought solution to the 4,6-desymmetrization of *myo*-inositol using asymmetric catalysis. Further mechanistic studies highlight a key single-electron reductive elimination in an enantioselective manner. This work opens the door for the development of transition-metal-catalysed enantioselective heteroatomic cross-coupling, which will ultimately benefit the synthetic community and related research areas.



## Online content

Any methods, additional references, Nature Portfolio reporting summaries, source data, extended data, supplementary information, acknowledgements, peer review information; details of author contributions and competing interests; and statements of data and code availability are available at <https://doi.org/10.1038/s41557-022-01102-z>.

## References

- de Meijere, A., Bräse, S. & Oestreich, M. (eds) *Metal-Catalyzed Cross-Coupling Reactions and More* (Wiley, 2014).
- Cherney, A. H., Kadunce, N. T. & Reisman, S. E. Enantioselective and enantiospecific transition-metal-catalyzed cross-coupling reactions of organometallic reagents to construct C–C bonds. *Chem. Rev.* **115**, 9587–9652 (2015).
- Choi, J. & Fu, G. C. Transition metal-catalyzed alkyl-alkyl bond formation: another dimension in cross-coupling chemistry. *Science* **356**, eaaf7230 (2017).
- Zhou, F., Liu, J. & Cai, Q. Transition metal catalyzed asymmetric aryl carbon-heteroatom bond coupling reactions. *Synlett* **27**, 664–675 (2016).
- Chinn, A. J., Kim, B., Kwon, Y. & Miller, S. J. Enantioselective intermolecular C–O bond formation in the desymmetrization of diarylmethines employing a guanidinylated peptide-based catalyst. *J. Am. Chem. Soc.* **139**, 18107–18114 (2017).
- Kainz, Q. M. et al. Asymmetric copper-catalyzed C–N cross-couplings induced by visible light. *Science* **351**, 681–684 (2016).
- Bartoszewicz, A., Matier, C. D. & Fu, G. C. Enantioconvergent alkylations of amines by alkyl electrophiles: copper-catalyzed nucleophilic substitutions of racemic  $\alpha$ -halolactams by indoles. *J. Am. Chem. Soc.* **141**, 14864–14869 (2019).
- Chen, C., Peters, J. C. & Fu, G. C. Photoinduced copper-catalysed asymmetric amidation via ligand cooperativity. *Nature* **596**, 250–256 (2021).
- Bai, J., Cui, X., Wang, H. & Wu, Y. Copper-catalyzed reductive coupling of aryl sulfonyl chlorides with *H*-phosphonates leading to *S*-aryl phosphorothioates. *Chem. Commun.* **50**, 8860–8863 (2014).
- Mulina, O. M., Ilovaisky, A. I. & Terent'ev, A. O. Oxidative coupling with S–N bond formation. *Eur. J. Org. Chem.* **2018**, 4648–4672 (2018).
- Mampuy, P., McElroy, C. R., Clark, J. H., Orru, R. V. A. & Maes, B. U. W. Thiosulfonates as emerging reactants: synthesis and applications. *Adv. Synth. Catal.* **362**, 3–64 (2020).
- Peng, K. & Dong, Z.-B. Recent advances in sulfur-centered S–X (X = N, P, O) bond formation catalyzed by transition metals. *Eur. J. Org. Chem.* **2020**, 5488–5495 (2020).
- Jang, H.-Y. Oxidative cross-coupling of thiols for S–X (X = S, N, O, P and C) bond formation: mechanistic aspects. *Org. Biomol. Chem.* **19**, 8656–8686 (2021).
- Korch, K. M. & Watson, D. A. Cross-coupling of heteroatomic electrophiles. *Chem. Rev.* **119**, 8192–8228 (2019).
- Hartwig, J. F., Shaughnessy, K. H., Shekhar, S. & Green, R. A. in *Organic Reactions* (ed. Denmark, S. E.) 853–958 (Wiley, 2020).
- Sambigao, C., Marsden, S. P., Blacker, A. J. & McGowan, P. C. Copper catalysed Ullmann type chemistry: from mechanistic aspects to modern development. *Chem. Soc. Rev.* **43**, 3525–3550 (2014).
- Elrod, L. T., Boxwala, H., Haq, H., Zhao, A. W. & Waterman, R. As–As bond formation via reductive elimination from a zirconocene bis(dimesitylarsenide) compound. *Organometallics* **31**, 5204–5207 (2012).
- Neumann, J. J., Suri, M. & Glorius, F. Efficient synthesis of pyrazoles: oxidative C–C/N–N bond-formation cascade. *Angew. Chem. Int. Ed.* **49**, 7790–7794 (2010).
- Kohl, S. W. et al. Consecutive thermal H<sub>2</sub> and light-induced O<sub>2</sub> evolution from water promoted by a metal complex. *Science* **324**, 74–77 (2009).
- Hartwig, J. F. Carbon–heteroatom bond formation catalysed by organometallic complexes. *Nature* **455**, 314–322 (2008).
- Torres, G. M., Liu, Y. & Arndtsen, B. A. A dual light-driven palladium catalyst: breaking the barriers in carbonylation reactions. *Science* **368**, 318–323 (2020).
- Cook, T. R., Surendranath, Y. & Nocera, D. G. Chlorine photoelimination from a diplatinum core: circumventing the back reaction. *J. Am. Chem. Soc.* **131**, 28–29 (2009).
- van Leest, N. P. et al. in *Advances in Organometallic Chemistry* (eds Pérez, P. J. et al.) 71–180 (Academic Press, 2018).
- Fang, C. et al. Mechanistically guided predictive models for ligand and initiator effects in copper-catalyzed atom transfer radical polymerization (Cu-ATRP). *J. Am. Chem. Soc.* **141**, 7486–7497 (2019).
- Wang, F.-L. et al. Mechanism-based ligand design for copper-catalysed enantioconvergent C(sp<sup>3</sup>)–C(sp) cross-coupling of tertiary electrophiles with alkynes. *Nat. Chem.* **14**, 949–957 (2022).
- Proctor, R. S. J., Colgan, A. C. & Phipps, R. J. Exploiting attractive non-covalent interactions for the enantioselective catalysis of reactions involving radical intermediates. *Nat. Chem.* **12**, 990–1004 (2020).
- Zhang, C., Li, Z.-L., Gu, Q.-S. & Liu, X.-Y. Catalytic enantioselective C(sp<sup>3</sup>)–H functionalization involving radical intermediates. *Nat. Commun.* **12**, 475 (2021).
- Beletskaya, I. & Moberg, C. Element–element additions to unsaturated carbon–carbon bonds catalyzed by transition metal complexes. *Chem. Rev.* **106**, 2320–2354 (2006).
- Waldman, A. J., Ng, T. L., Wang, P. & Balskus, E. P. Heteroatom–heteroatom bond formation in natural product biosynthesis. *Chem. Rev.* **117**, 5784–5863 (2017).
- Ertl, P., Altmann, E. & McKenna, J. M. The most common functional groups in bioactive molecules and how their popularity has evolved over time. *J. Med. Chem.* **63**, 8408–8418 (2020).
- Leitao, E. M., Jurca, T. & Manners, I. Catalysis in service of main group chemistry offers a versatile approach to *p*-block molecules and materials. *Nat. Chem.* **5**, 817–829 (2013).
- Melen, R. L. Frontiers in molecular *p*-block chemistry: from structure to reactivity. *Science* **363**, 479–484 (2019).
- Gu, Q.-S., Li, Z.-L. & Liu, X.-Y. Copper(I)-catalyzed asymmetric reactions involving radicals. *Acc. Chem. Res.* **53**, 170–181 (2020).
- Dong, X.-Y. et al. A general asymmetric copper-catalysed Sonogashira C(sp<sup>3</sup>)–C(sp) coupling. *Nat. Chem.* **11**, 1158–1166 (2019).
- Glass, R. S. Sulfur radicals and their application. *Top. Curr. Chem.* **376**, 22 (2018).
- Patai, S. & Rappoport, Z. (eds) *The Chemistry of Sulphonic Acids, Esters and Their Derivatives* (Wiley, 1991).
- Nájera, C., Foubelo, F., Sansano, J. M. & Yus, M. Enantioselective desymmetrization reactions in asymmetric catalysis. *Tetrahedron* **106–107**, 132629 (2022).
- Feng, J., Holmes, M. & Krische, M. J. Acyclic quaternary carbon stereocenters via enantioselective transition metal catalysis. *Chem. Rev.* **117**, 12564–12580 (2017).
- Lee, J. Y., You, Y. S. & Kang, S. H. Asymmetric synthesis of all-carbon quaternary stereocenters via desymmetrization of 2,2-disubstituted 1,3-propanediols. *J. Am. Chem. Soc.* **133**, 1772–1774 (2011).
- Tsuda, Y., Kuriyama, M. & Onomura, O. Synthesis of optically active oxazoline derivatives via catalytic asymmetric desymmetrization of 1,3-diols. *Chem. Eur. J.* **18**, 2481–2483 (2012).

41. Yamamoto, K., Tsuda, Y., Kuriyama, M., Demizu, Y. & Onomura, O. Copper-catalyzed enantioselective synthesis of oxazolines from aminotriols via asymmetric desymmetrization. *Chem. Asian J.* **15**, 840–844 (2020).
42. Hong, M. S., Kim, T. W., Jung, B. & Kang, S. H. Enantioselective formation of *tert*-alkylamines by desymmetrization of 2-substituted serinols. *Chem. Eur. J.* **14**, 3290–3296 (2008).
43. You, Y. S., Kim, T. W. & Kang, S. H. Asymmetric formation of *tert*-alkylamines from serinols by a dual function catalyst. *Chem. Commun.* **49**, 9669–9671 (2013).
44. Jung, B., Hong, M. S. & Kang, S. H. Enantioselective synthesis of tertiary alcohols by the desymmetrizing benzylation of 2-substituted glycerols. *Angew. Chem. Int. Ed.* **46**, 2616–2618 (2007).
45. Jung, B. & Kang, S. H. Chiral imine copper chloride-catalyzed enantioselective desymmetrization of 2-substituted 1,2,3-propanetriols. *Proc. Natl Acad. Sci. USA* **104**, 1471–1475 (2007).
46. You, Z., Hoveyda, A. H. & Snapper, M. L. Catalytic enantioselective silylation of acyclic and cyclic triols: application to total syntheses of clerodindicins D, F and C. *Angew. Chem. Int. Ed.* **48**, 547–550 (2009).
47. Manville, N., Alite, H., Haeffner, F., Hoveyda, A. H. & Snapper, M. L. Enantioselective silyl protection of alcohols promoted by a combination of chiral and achiral Lewis basic catalysts. *Nat. Chem.* **5**, 768–774 (2013).
48. Yasohara, Y., Miyamoto, K., Kizaki, N., Hasegawa, J. & Ohashi, T. A practical chemoenzymatic synthesis of a key intermediate of antifungal agents. *Tetrahedron Lett.* **42**, 3331–3333 (2001).
49. Mota, C. J. A., Pinto, B. P. & de Lima, A. L. *Glycerol: A Versatile Renewable Feedstock for the Chemical Industry* (Springer, 2017).
50. Giustra, Z. X. & Tan, K. L. The efficient desymmetrization of glycerol using scaffolding catalysis. *Chem. Commun.* **49**, 4370–4372 (2013).
51. Thomas, M. P., Mills, S. J. & Potter, B. V. L. The ‘other’ inositols and their phosphates: synthesis, biology and medicine (with recent advances in *myo*-inositol chemistry). *Angew. Chem. Int. Ed.* **55**, 1614–1650 (2016).
52. Metrano, A. J. & Miller, S. J. Peptide-based catalysts reach the outer sphere through remote desymmetrization and atroposelectivity. *Acc. Chem. Res.* **52**, 199–215 (2019).
53. Fiori, K. W., Puchlopek, A. L. A. & Miller, S. J. Enantioselective sulfonylation reactions mediated by a tetrapeptide catalyst. *Nat. Chem.* **1**, 630–634 (2009).
54. Jordan, P. A., Kayser-Bricker, K. J. & Miller, S. J. Asymmetric phosphorylation through catalytic P(III) phosphoramidite transfer: enantioselective synthesis of D-*myo*-inositol-6-phosphate. *Proc. Natl Acad. Sci. USA* **107**, 20620–20624 (2010).
55. Russell, G. A., Tashtoush, H. & Ngoviwatchai, P. Alkylation of  $\beta$ -substituted styrenes by a free radical addition-elimination sequence. *J. Am. Chem. Soc.* **106**, 4622–4623 (1984).
56. Truce, W. E. & Heuring, D. L. Preparation and photodecomposition of  $\alpha$ -toluenesulfonyl iodide. *J. Org. Chem.* **39**, 245–246 (1974).
57. King, J. F., Lam, J. Y. L. & Skonieczny, S. Mechanisms of hydrolysis and related nucleophilic displacement reactions of alkanesulfonyl chlorides: pH dependence and the mechanism of hydration of sulfenes. *J. Am. Chem. Soc.* **114**, 1743–1749 (1992).
58. Demizu, Y., Matsumoto, K., Onomura, O. & Matsumura, Y. Copper complex catalyzed asymmetric monosulfonylation of *meso*-*vic*-diols. *Tetrahedron Lett.* **48**, 7605–7609 (2007).
59. Xu, J. et al. Remote C–H activation of quinolines through copper-catalyzed radical cross-coupling. *Chem. Asian J.* **11**, 882–892 (2016).

**Publisher's note** Springer Nature remains neutral with regard to jurisdictional claims in published maps and institutional affiliations.

Springer Nature or its licensor (e.g. a society or other partner) holds exclusive rights to this article under a publishing agreement with the author(s) or other rightsholder(s); author self-archiving of the accepted manuscript version of this article is solely governed by the terms of such publishing agreement and applicable law.

© The Author(s), under exclusive licence to Springer Nature Limited 2022

## Methods

### Synthesis of 1–32, 47–55 and 60

Under an Ar atmosphere, an oven-dried resealable Schlenk tube equipped with a magnetic stirring bar was charged with CuI (10 mol%), **L\*4** (10 mol%), Ag<sub>2</sub>CO<sub>3</sub> (0.60 equiv.), proton sponge (20 mol%), diols (0.30 mmol, 1.0 equiv.) or glycerol (1.0 g, 11 mmol, 1.0 equiv.) and anhydrous CHCl<sub>3</sub> (0.10 M). The corresponding sulfonyl chloride (1.2 equiv.) was added and the reaction mixture was stirred at 0 °C or room temperature (r.t.). Upon completion (monitored by thin-layer chromatography), the reaction mixture was concentrated in vacuo and the residue was purified by column chromatography on silica gel to afford the desired product.

### Synthesis of 33–43

Under an Ar atmosphere, an oven-dried resealable Schlenk tube equipped with a magnetic stirring bar was charged with CuCl (10 mol%), **L\*8** or **L\*9** (10 mol%), Ag<sub>2</sub>CO<sub>3</sub> (0.60 equiv.), proton sponge (0 or 5.0 mol%), diols (0.20 mmol, 1.0 equiv.) and anhydrous CHCl<sub>3</sub> (0.10 M), then 4-methoxybenzenesulfonyl chloride (1.2 equiv.) was added and the reaction mixture was stirred at r.t. Upon completion (monitored by thin-layer chromatography), the reaction mixture was concentrated in vacuo and the residue was purified by column chromatography on basic aluminium oxide to afford the desired product.

### Synthesis of 67

Under an Ar atmosphere, an oven-dried resealable Schlenk tube equipped with a magnetic stirring bar was charged with CuBr·SMe<sub>2</sub> (10 mol%), **L\*10** (15 mol%), Ag<sub>2</sub>CO<sub>3</sub> (0.60 equiv.), **A-3** (58.0 mg, 0.20 mmol, 1.0 equiv.) and anhydrous CHCl<sub>3</sub> (0.10 M), then benzenesulfonyl chloride (1.2 equiv.) was added and the reaction mixture was stirred at r.t. for 2 d. Upon completion, the reaction mixture was concentrated in vacuo and the residue was purified by column chromatography on silica gel to afford the desired product **67** (64.2 mg, 75% yield, 97% e.e.).

### Synthesis of 68

Under an Ar atmosphere, an oven-dried resealable Schlenk tube equipped with a magnetic stirring bar was charged with CuBH<sub>4</sub>(PPh<sub>3</sub>)<sub>2</sub> (10 mol%), **L\*4** (15 mol%), Ag<sub>2</sub>CO<sub>3</sub> (0.60 equiv.), **A-4** (0.20 mmol, 1.0 equiv.) and anhydrous CH<sub>2</sub>Cl<sub>2</sub> (0.10 M), then benzenesulfonyl chloride (1.2 equiv.) was added and the reaction mixture was stirred at room temperature for 3 d. Upon completion, the reaction mixture was concentrated in vacuo and the residue was purified by column chromatography on silica gel to afford the desired product **68** (78.3 mg, 85% yield, 93% e.e.).

### Synthesis of 69

Under an Ar atmosphere, an oven-dried resealable Schlenk tube equipped with a magnetic stirring bar was charged with CuBH<sub>4</sub>(PPh<sub>3</sub>)<sub>2</sub> (10 mol%), **L\*11** (12 mol%), Ag<sub>2</sub>CO<sub>3</sub> (0.60 equiv.), **A-5** (2.6 mmol, 1.0 equiv.), 4 Å MS (0.40 g) and anhydrous CHCl<sub>3</sub> (0.050 M), then benzenesulfonyl chloride (1.2 equiv.) was added and the reaction mixture was stirred at r.t. for 2 d. The reaction mixture was filtered through a plug of celite (rinsed with EtOAc) and concentrated in vacuo. The residue was purified by column chromatography on silica gel to afford the desired product **69** (1.07 g, 78% yield, 91% e.e.).

## Data availability

The data that support the findings of this study are available within the paper and its Supplementary Information. Crystallographic data for the structures reported in this Article have been deposited at the Cambridge Crystallographic Data Centre, under deposition numbers CCDC [2102449 \(L\\*4\)](#), [2102446 \(16\)](#), [2102451 \(45\)](#), [2102448 \(59\)](#), [2102450 \(69\)](#) and [2102452 \(72\)](#). Copies of the data can be obtained free of charge via <https://www.ccdc.cam.ac.uk/structures/>.

## Acknowledgements

We appreciate the help of W. Jiang and his colleagues from SUSTech for enantiopurity characterization, and the assistance of SUSTech Core Research Facilities. Financial support from the National Key R&D Program of China (nos. 2021YFF0701604 and 2021YFF0701704, X.-Y.L.), the National Natural Science Foundation of China (nos. 22025103, 92256301, and 21831002, X.-Y.L.; 22001111, Y.-F.C.; 22001109 and 22271133, Q.-S.G.; 21873081 and 22122109, X.H.), the Guangdong Innovative Program (no. 2019BT02Y335, X.-Y.L.), Guangdong Provincial Key Laboratory of Catalysis (no. 2020B121201002, X.-Y.L.), Shenzhen Science and Technology Program (nos. KQTD20210811090112004, X.-Y.L. and Q.-S.G.; JCYJ20200109141001789, X.-Y.L.), the Starry Night Science Fund of Zhejiang University Shanghai Institute for Advanced Study (no. SN-ZJU-SIAS-006, X.H.), Beijing National Laboratory for Molecular Sciences (no. BNLMS202102, X.H.), CAS Youth Interdisciplinary Team (no. JCTD-2021-11, X.H.), Fundamental Research Funds for the Central Universities (nos. 226-2022-00140 and 226-2022-00224, X.H.), the Center of Chemistry for Frontier Technologies and Key Laboratory of Precise Synthesis of Functional Molecules of Zhejiang Province (no. PSFM2021-01, X.H.) and the State Key Laboratory of Clean Energy Utilization (no. ZJUCEU2020007, X.H.) is gratefully acknowledged.

## Author contributions

Y.-F.C., Z.-L.Y. and Y.T. designed the experiments and analysed the data. Y.-F.C., Z.-L.Y., Y.T., H.-T.W., N.-C.J., J.-Q.B., D.-T.X. and Z.-L.L. performed the experiments. X.H. designed the DFT calculations. J.-R.L. and G.-X.X. performed the DFT calculations. All authors participated in writing the manuscript. Q.-S.G. and X.-Y.L. conceived of and supervised the project.

## Competing interests

The authors declare no competing interests.

## Additional information

**Supplementary information** The online version contains supplementary material available at <https://doi.org/10.1038/s41557-022-01102-z>.

**Correspondence and requests for materials** should be addressed to Qiang-Shuai Gu, Xin Hong or Xin-Yuan Liu.

**Peer review information** *Nature Chemistry* thanks Hye-Young Jang, Allan Watson and Yanying Zhao for their contribution to the peer review of this work.

**Reprints and permissions information** is available at [www.nature.com/reprints](http://www.nature.com/reprints).